A new geological model for Spriana landslide

L. Longoni · M. Papini · D. Arosio · L. Zanzi · D. Brambilla

Received: 21 February 2013 / Accepted: 3 April 2014 / Published online: 22 April 2014

L. Longoni (✉) · M. Papini · D. Arosio · L. Zanzi · D. Brambilla
Dipartimento di Ingegneria Civile e Ambientale, Politecnico di Milano, Piazza Leonardo da Vinci, 32, 20133 Milan, Italy
e-mail: laura.longoni@polimi.it

Introduction

Many landslides in the Alpine area involve large volumes of material and can be classified as complex landslides (Cruden and Varnes 1996). These mass movements may display different kinematic behaviours ranging from creep to fast movements, and include rockfall, rock slides, debris flows, etc. Also the involved materials can be very diverse, with rocks or soils with various grain sizes and percentages of water content. Moreover, sometimes these large mass movements can evolve into rock-debris avalanches, becoming catastrophic failures characterized by high velocity (Revellino et al. 2004; Catane et al. 2008; Futalan et al. 2010; Gattinoni et al. 2012). Unfortunately, their prediction is still a challenge to scientists dealing with landslide hazards.

Common assessment methods are based on empirical and numerical approaches (Aleotti and Chowdury 1999; Dai et al. 2002; Hungr et al. 2005). None of these can be easily applied to complex landslides, due to the high spatial and temporal variability of input parameters (Einstein 1988; Scavia et al. 1990). The empirical methods provide a quick evaluation of mass movement (Scheiddeger 1973; Howard 1973; Hsu 1975; Tian Chi 1983; Tommasi et al. 2008), but the complexity of the assessment of this type of landslide may result in a rough outcome (Crosta et al. 2003). Instead, thanks to remarkable advances, numerical modelling often allows for the achievement of satisfactory results (Jing and Hudson 2002), despite the uncertainty related to the definition of input parameters (Welkner et al. 2010; Eberhardt et al. 2004; Stead et al. 2006).

Numerical modelling is considered the most promising tool to study slope instability. As a matter of fact, numerical codes, based on either continuous or discrete

approaches, may help us to better understand failure mechanisms and deformation processes. As stated above, the continuous changes in kinematic behaviour make simulation of large landslides pretty challenging. Therefore, the choice of code depends on the specific problem to solve or to analyse, e.g., the analysis of the deeper surface of failure, the study of the slide kinematics, and so on.

Known modelling methods for discontinuous media can be split into two classes (Tommasi et al. 2008): discontinuous deformation analysis (DDA; Shi 1988) and distinct elements methods (DEM; Cundall 1971). Literature provides many applications of DEM to complex landslides (Campbell et al. 1995; Calvetti et al. 2000; Tommasi et al. 2003; Marcato et al. 2005; Welkner et al. 2010; Brideau et al. 2012), whereas there are fewer applications of DDA methods (Koo and Chern 1998; Fukawa et al. 2005). On the other hand, many authors use methods that consider continuous media and have different approaches according to the rheological model (Savage and Hutter 1989; Crosta et al. 2001, 2003; Gonzales et al. 2003; Pirulli 2009; Discenza et al. 2011). In both continuous and discrete models, the complexity of the slope assessment coupled with the exceptional velocity in the case of rock-debris avalanche is hard to explain by the use of a unique model.

Despite the progress in numerical modelling, the uncertainty in physical model reconstruction has important consequences in numerical outcomes (Welkner et al. 2010). The integration of all available information through multidisciplinary approaches (Bonnard et al. 2004) can provide all the features that play an important role in slope behaviour, avoiding considerable simplifications in the slope assessment phase.

This paper focuses on the complex landslide of Spriana, a small village located in Valmalenco Valley in the Central Alps, few kilometres north of the city of Sondrio (Fig. 1). The investigated mass movement may evolve in a rock-debris avalanche and cause several damages to man-made structures. The authors review previous geological and geophysical investigations, starting from the geological interpretation provided by Belloni and Gandolfo (1997). A large amount of data has been analysed in order to perform a detailed characterization of the slope; laboratory and drilling tests, geophysical investigations, monitoring data and field analysis were integrated to define the geological model. After the description of the slope assessment, numerical modelling is discussed. According to the considerations listed above, continuous and discrete approaches have been tested on the case study in order to determine the best fit to the observed landslide behaviour.

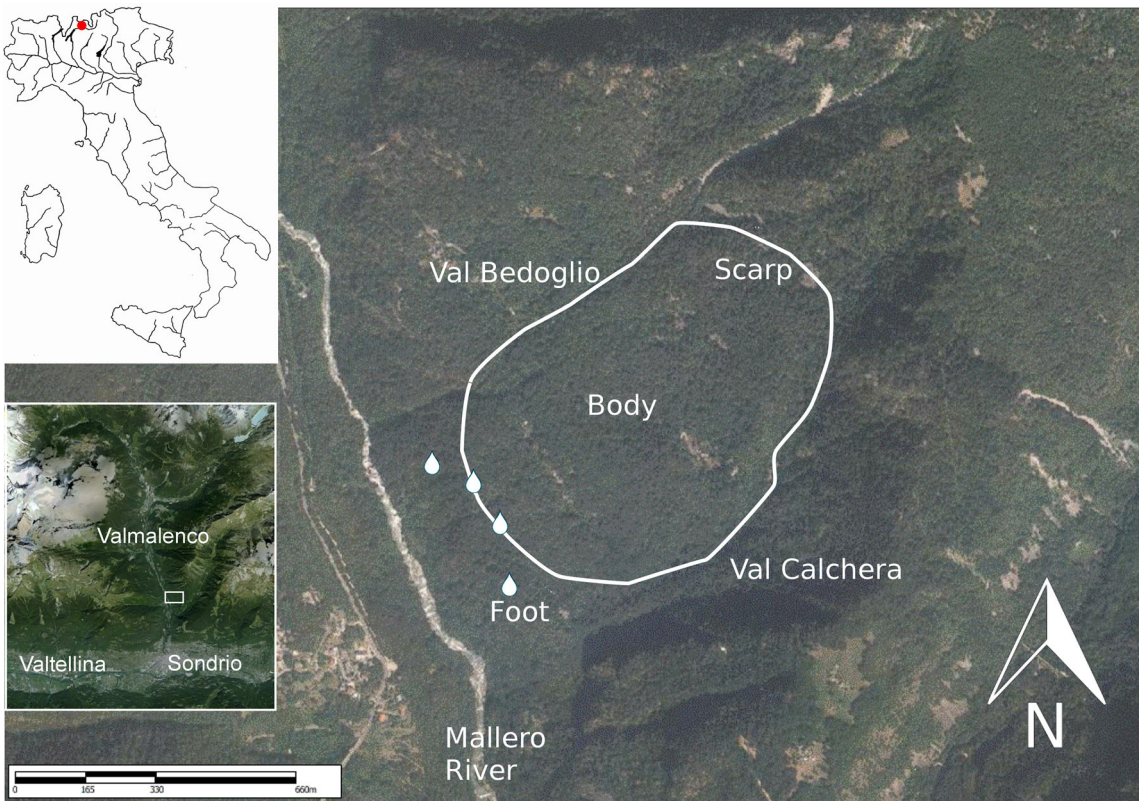

Fig. 1 Location of the investigated site. The boundary of Spriana landslide is *outlined* and *white drops* represent the water springs

Spriana complex landslide

Spriana landslide is considered the most important instability in Valmalenco, a valley in the Italian Central Alps with a North–South trend and which is crossed by the Mallero river. The landslide is located on the left bank of Valmalenco, just 1 km south of the residential area of Spriana village and about 4 km upstream of the city of Sondrio, where the valley flows into Valtellina Valley (Fig. 1).

This mass movement has been studied by many authors since the early 19th century because of its extent and geographic position (Brugner 1961, 1963, 1964; Cancelli et al. 1979; Belloni and Gandolfo 1997; Papini et al. 2005; Longoni et al. 2013). Significant displacements have been observed since the beginning of the last century. Several investigations were carried out after the massive 1987 flood that affected the entire Valtellina Valley, and aimed to improve the knowledge of the instability, as well as to support the project of a by-pass tunnel able to divert Mallero river discharge in case of slope failure. Significant movements of about 2–3 m, mainly clustered in the lower section of the slope, were registered between 1977 and 1978 as a consequence of heavy rainfalls; successively no movement was recorded till the end of 1989. According to the topographic monitoring data, the landslide did not seem to move significantly during the 1987 flood event (ISMES 1990a, b). In the late 1980s, 18 continuous coring boreholes were performed across the slope with an explored depth spanning from 30 to 200 m. Afterwards, a monitoring system was installed, holes were used for piezometric readings on a regular basis, and in addition, five holes were equipped with inclinometer sensors. Furthermore, in 1989, a sub-horizontal 150 m-long 2 m-wide explorative tunnel was drilled at an elevation of 1,041 m asl, in order to directly inspect the geological features of the landslide body. In fact, fractured rock can be observed along the entire tunnel apart from the last 5 m, where fresh rock is present.

The most comprehensive analysis of the Spriana landslide has been presented by Belloni and Gandolfo (1997), and it is shortly summarized here. From a geological point of view, the slope is composed of gneiss and mica schist belonging to the Gneiss formation of Monte Canale, covered by landslide debris and glacial deposits. According to the geological evolution involving the Valmalenco Valley, paraglacial stress release conditioned the rock slope instability of Spriana (Belloni and Gandolfo 1997). Slope debuttressing produced an intense state of fracturation to depths down to 100 m, with the presence of breccias and slickensides in the rock mass (Cancelli 1986; Ballantyne 2002). The unstable mass covers an area of 0.60 km^2 and is bounded on the northwest by Bedoglio Valley and on the southeast by Calchera Valley (Fig. 1). In the higher section of the slope, two scarps can be found: the first one at 1,100 m asl and the second at 1,400 m asl, probably positioned on a faults set with attitude 240°/80°, as remarked by field evidence and by previous works. Morphological evidences indicate that instability might affect the slope even at higher altitudes, up to 1,700 m asl. The presence of perennial water springs suggests to locate the landslide foot between 700 m and 750 m asl, approximately 200 m above the bottom of the valley (placed at about 500 m asl) (Fig. 1). Piezometric data sets have shown that groundwater surface in the lower part of the slope is placed at about 900 m asl. This groundwater system seems to have a high accumulation volume inside the slope; therefore, it can feed the array of springs located 200 m downslope. In the upper section, the water percolates in depth, thanks to the permeability of the superficial debris, and tends to gather at the interface between fractured and low permeability rock. It is believed that an increase of the groundwater level due to rainfalls and snowmelt might trigger the instability mechanism. Considering the geomorphological and geological features of the slope and the volumes involved, a possible collapse of the slope might originate a rock-debris avalanche with relevant downstream consequences. Indeed, the displaced material might occlude the riverbed, creating a natural dam reaching heights ranging from 70 to 100 m (ISMES 1990a, b).

Although the work of Belloni and Gandolfo (1997) is remarkable and well organized, the characterization of the deeper shear surface of the landslide, i.e., the position as well as the continuity of the surface of failure, is still a challenge. In the following paragraph, we try to develop a thorough physical model of the slope, accounting for results of previous investigations and newly available monitoring data sets supplied by Regional Agency for the Environment (ARPA).

The physical model

Interpretation of recent monitoring data

Important displacements took place again during Spring 2001, and were probably caused by snowmelt water along with heavy and prolonged rainfalls that occurred during the previous autumn. Until 2006, no other notable movements were recorded. The analysis of the monitoring data sets up to 2006 is described in an unpublished internal report produced by the authors together with ARPA technicians. Since collected data sets are covered by a confidentiality agreement, only the fundamental features of the report are presented here.

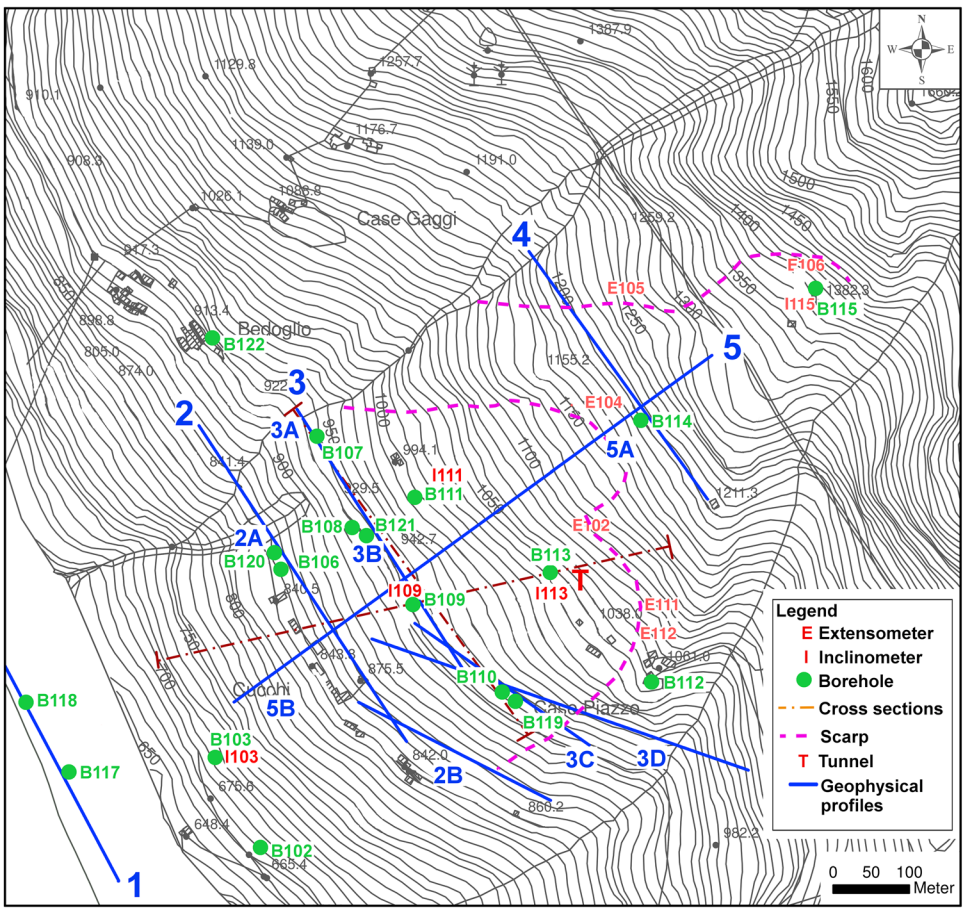

Fig. 2 Topographic map with boreholes, geotechnical monitoring network, explorative tunnel and seismic refraction profiles. Landslide scarps and position of cross-sections of Fig. 3 are also shown (modified after ISMES 1990a, b)

Monitoring data related to the 2001 events can provide new hints to improve the understanding of the kinematic behaviour of the slope, as well as of disregarded geological details. As far as meteorological parameters are concerned, data analysis showed that rainfalls in 2001 are comparable to rainfalls related to the 1977 event. It was found out that Spriana slope is susceptible to a peak of cumulative rainfall after rainy months. During Winter 2000–2001, maximum thickness of the snow cover was measured to be around 0.9 m and consequently snowmelt water also contributed to increase the groundwater level. Extensometer and borehole inclinometer readings were analyzed for that which concerns the geotechnical monitoring system, (Fig. 2). The displacements recorded by the extensometers from 1990 to 2004 reveal that:

- Extensometer E106 recorded the highest cumulative displacement (as a matter of fact, it is located on the main scarp at 1,400 m asl);
- Extensometers E106 and E105, both located on the main scarp, showed continuous displacements during the considered period;
- Extensometer E102 recorded a cumulative displacement that is double compared to that recorded by extensometers E103 and E104;
- Extensometers E111, E112, E102 showed a peak in the cumulative displacement in correspondence with the rainfall event (in Spring 2001);
- Extensometers E104 and E103 showed low but continuous cumulative displacements during the study period.

Internal displacement of the rock mass was monitored by means of boreholes equipped with inclinometers. However, it has to be stated that due to the short-term sustainability of the inclinometer system, few data are available. Interpretation of collected data sets can be summarized as follows:

- Inclinometer readings reveal the presence of two failure surfaces: the first one is along the contact between debris and fractured rocks, and it was already well-known (Belloni and Gandolfo 1997); the second one is deeper and is located within the most fractured rock layer (commonly at depths between 50 and 100 m);
- The greatest displacement was recorded by I113, near Calchera Valley. Considering the inclinometers located across the slope at similar elevations (I113, I109 and I111), displacements seem to decrease when approaching Bedoglio Valley (I109 and then I111);

- The analysis of I113 and I103 data sets between 2001 and 2004 shows greater displacements in the upper part of the slope.

According to extensometer and inclinometer data listed above, and considering uncertainties due to manual registration and to the relatively short study period, the authors together with the ARPA technicians conceived a new hypothesis about the slope behavior, focusing on the role of the deeper failure surface. Two different responses to rainfalls and snowmelt water have been observed, depending on the position on the slope. The measurement stations near Calchera Valley react almost immediately to rainfall and snowmelt inputs. This behaviour suggests the presence of a geological setting prone to instability. On the other hand, geotechnical monitoring tools deployed close to Bedoglio Valley indicate that the northern section of the landslide body shows smaller but continuous displacements.

Analysis of the monitoring data sets of Spriana landslide has allowed for the observation of some features of landslide behaviour that would otherwise have gone unnoticed. Global slope response suggests the presence of a complex failure mechanism that seems to be controlled by a twofold deep failure surface. This hypothesis is further investigated in the following by reprocessing the available data sets, focusing on the shape and characterization of the deeper sliding surface.

Review of the geological setting

To begin with, boreholes (performed by ISMES in 1990a, b) were carefully reviewed in order to determine the most promising locations to perform meaningful geological cross-sections, addressing particularly the deeper failure surface. Previous information from the corings and from the explorative tunnel was integrated with a new extensive field investigation. Standard geological and structural surveys were performed both on the slope outcrops and inside the explorative tunnel. Discontinuities were characterized in the field according to ISRM (1978). Figure 3 depicts a simplified geological cross-section across boreholes 107, 108, 109 and 110 (Fig. 2), and a cross-section intercepting the explorative tunnel and oriented parallel to the likely direction of the landslide movement. The shallow failure surface along the interface between debris and fractured rock is typically located at depths ranging from 12 to 40 m (Cancelli 1986; Belloni and Gandolfo 1997). This is in agreement with displacement data collected by the inclinometers. In addition, direct inspection of the tunnel pinpointed a thin debris layer with a silty-sandy matrix containing clay along this first interface. Therefore, the instability might also be ascribed to the presence of this silty material. The cross-sections illustrate a brecciated layer that probably identifies a shear zone within which a deeper failure surface may be located (Fig. 3). The complex geological setting related to this deeper surface of failure deserves a detailed analysis considering all available pieces of information. As far as corings are concerned, borehole logs close to Calchera Valley (102, 103, 109, 110, 119, 113—see Fig. 2) generally include a layer of strongly brecciated gneiss with a thickness spanning from 5 to 35 m. Conversely, in the boreholes close to Bedoglio Valley, the fractured layer is described only as brecciated. Regarding the explorative tunnel, only 140 m could be inspected because of a collapse affecting the last 10 m. Several faults, mainly sub-vertical, were identified by the structural survey, while the geological survey detected very

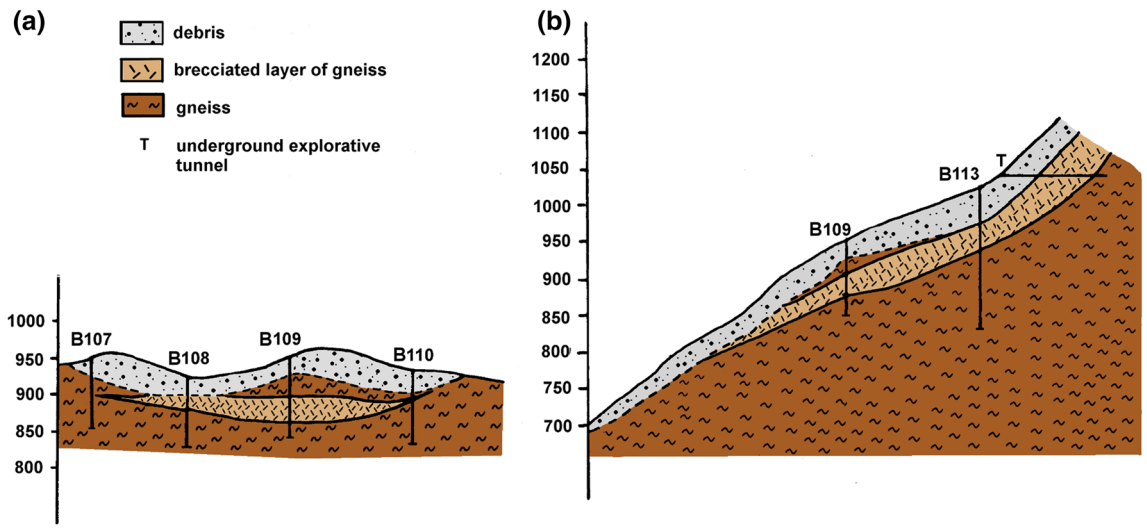

Fig. 3 **a** Cross-section along NW–SE direction; **b** cross-section approximately along the NE–SW direction

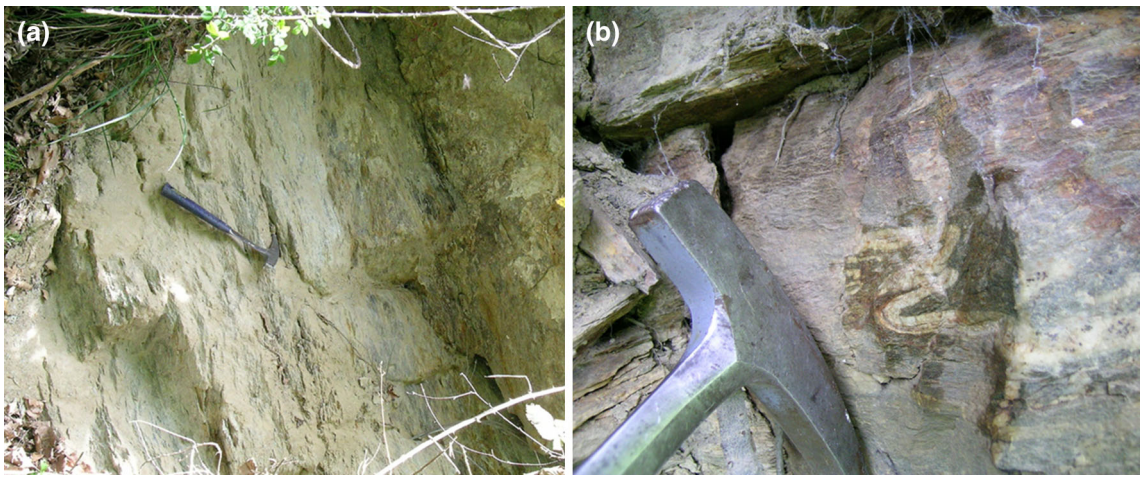

Fig. 4 **a** Strongly brecciated outcrop; **b** asymmetric fold

brecciated rocks from 130 m until the end of the tunnel. In this last section, a fault-gouge cataclastic zone with dip direction of 260° and inclination of 25°–30° was found (see also ISMES 1990a, b). By cross-correlating the abovementioned pieces of information, we decided to model the fault zone as a planar element (260°/25°–30°). Quite surprisingly, the plane is well in agreement with all collected data sets and geological evidences on the slope. The plane intersects the boreholes 113, 110, 109 and 102 approximately in correspondence with the strongly brecciated gneiss layer and the slope at about 700 m asl, where water springs were detected and were interpreted as the foot of the landslide (see paragraph 2). In addition, the plane outcrops a bit north of Calchera Valley, in agreement with the landslide boundary suggested by Belloni and Gandolfo (1997) and the presence of brecciated rock starting from the top of borehole 112. As a further validation, an ad hoc field investigation near Calchera Valley located a strongly brecciated outcrop and the geological analysis revealed asymmetric folds developed within the rock mass (Fig. 4), typical of shear zones.

Moving progressively northwards across the landslide body, the failure surface located within the strongly brecciated gneiss layer seems to get a bit deeper, and after reaching its maximum depth in the middle area of the landslide, it becomes shallower near Bedoglio Valley (Fig. 3). On this side, borehole logs indicate a weak layer of brecciated rock lying over partially weathered bedrock. The interface between these layers is deemed to be the deeper sliding surface affecting the northern section of the landslide and has a dip direction ranging from 160° to 180° and an inclination of 10°–30°.

According to the abovementioned considerations, the complex deeper surface of failure seems to be characterized by a wedge shape, due to the intersection of two weak layers with different structural framework features. The failure surface affecting the northern section of the slope (i.e., close to Bedoglio Valley) may be attributable to the glacial activity (Belloni and Gandolfo 1997; Ballantyne 2002), while the failure surface affecting the southern section of the slope (i.e., close to Calchera Valley) may be attributable to a fault zone. The update geological model of Spriana landslide has wedge-like surface of failure, as depicted in Fig. 5.

Geophysical investigation

To validate the hypothesis about the wedge shape of the failure surface and possibly to better constrain the geometry of the sliding planes, it was decided to process again the geophysical data sets collected in 1989 by Geo Prospecting SRL (1990). They performed a classical seismic refraction survey (Telford et al. 1990) along explorative different seismic spreads deployed across the slope along different orientations (Fig. 2). A 24-channel seismograph was used to record digital data, the spacing between geophones along each spread was 10 m and seismic sources were small dynamite charges placed in shallow (1–1.5 m deep) holes. After first arrival picking, time–distance curves were interpreted according to the Generalized Reciprocal Method (GRM; Palmer 1981). A two-layer structure was generally assumed, but the interpretation of the time–distance curves was often difficult due to rough changes in layer thickness and lateral variations of velocity. In some cases, a three-layer structure could have also been supposed. To avoid the tricky choice of sections of time–distance curves to be assigned to different subsurface layers, we processed picked first arrivals by means of refraction travel-time tomography (e.g., Phillips and Fehler 1991). According to this methodology, subsurface velocity

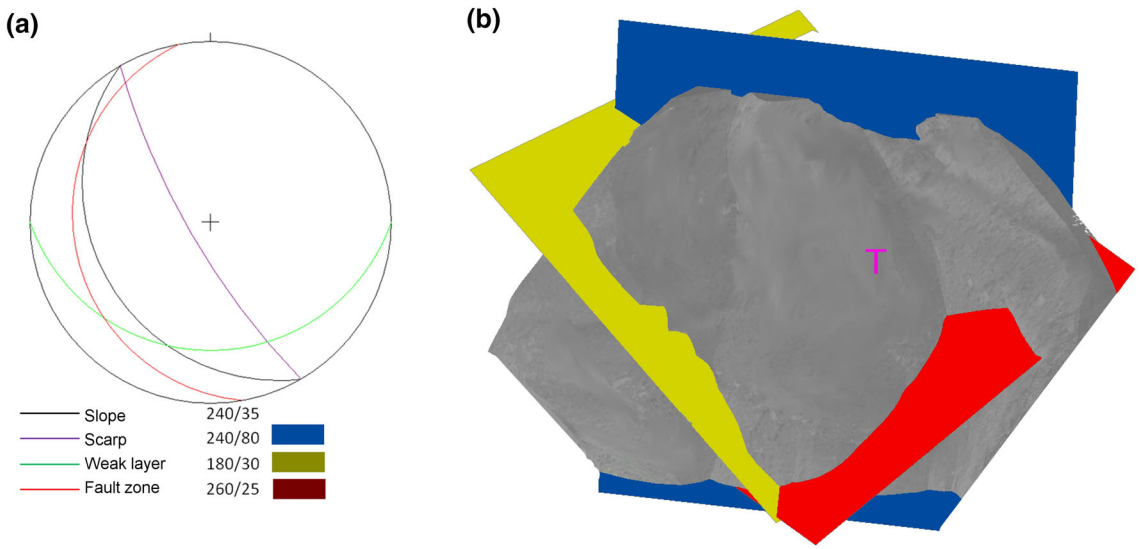

Fig. 5 **a** Stereographic representation of discontinuities; **b** image of the physical model based on the found discontinuity planes (*T* pinpoints the position of the explorative tunnel)

model is iteratively modified until a satisfactory match between synthetic (i.e., calculated) and real (i.e., picked) travel times is obtained. Here, we focus on spreads two and three, because they cross the landslide body approximately along the north–south direction, and therefore are promising to identify the wedge shape of the deeper failure surface. At first, the outcomes of the GRM method were taken as initial models for the tomographic inversions. Subsequently, to reduce the constraints of the tomographic inversion and to explore the stability of the final model, single-layer models with different velocity vertical gradients (generally ranging from 45 to 75 s^{-1}) were tested.

Figure 6 presents the final results relative to profiles 2A and 3A–3B, concerning the northern section of the slope, along with results relative to profiles 2B and 3D, concerning the southern section of the slope. In all the velocity maps, it is quite simple to identify a low velocity layer (dark blue area), followed by an intermediate velocity layer (light blue area) and a sudden increase of velocity up to 6,000 m/s (yellow–red area). This interpretation is also supported by borehole logs (where available). Considering the position of the seismic profiles on the slope (Fig. 2), a high velocity structure with a well-defined trend is clearly observable in the velocity sections. This structure seems to outcrop approximately at the boundaries of the unstable body (near Bedoglio Valley and Calchera Valley), and increases its depth when moving towards the central section of the slope. For these grounds, we interpreted the contact between this structure and the layer above as the wedge-shaped failure surface. In order to determine the attitude of the planes composing this contact, we picked possible interfaces corresponding to a velocity of 3,250 m/s on the velocity sections (Fig. 6) and interpolated the picked traces. We obtained two planes with attitudes 251°/29° and 200°/35° that reasonably support the assumptions provided by the review of the geological setting.

Numerical modelling

Once a reliable characterization of the physical model has been achieved, numerical simulations may allow a better understanding of the triggering factors and of the failure mechanisms. Three-dimensional codes have been used to explore the role and the importance of shear surface geometry on the landslide mechanism. As stated in the introduction, several applications for large landslides are based on both continuous and discontinuous approaches. Continuous modelling is used when rock mass is either massive or so fractured and weathered that it behaves almost like loose material. Discontinuous numerical models are used if kinematic behaviour is ruled by rock joints. In the latter case, there are two possible behaviors for each rock block: in simpler models, the blocks can be considered as rigid; whereas in more complex cases, blocks are considered to be deformable. According to the complexity of the shear surface of Spriana landslide, we deemed it reasonable to test both codes. Indeed, the presence of very fractured rocks would require the use of continuous methods, but as the slope is affected by faults and weakness surfaces, discontinuous methods would better constrain the analysis of the wedge-shaped surface. Using three-dimensional codes, we performed a back-analysis of the 2001 event by reproducing the groundwater level recorded

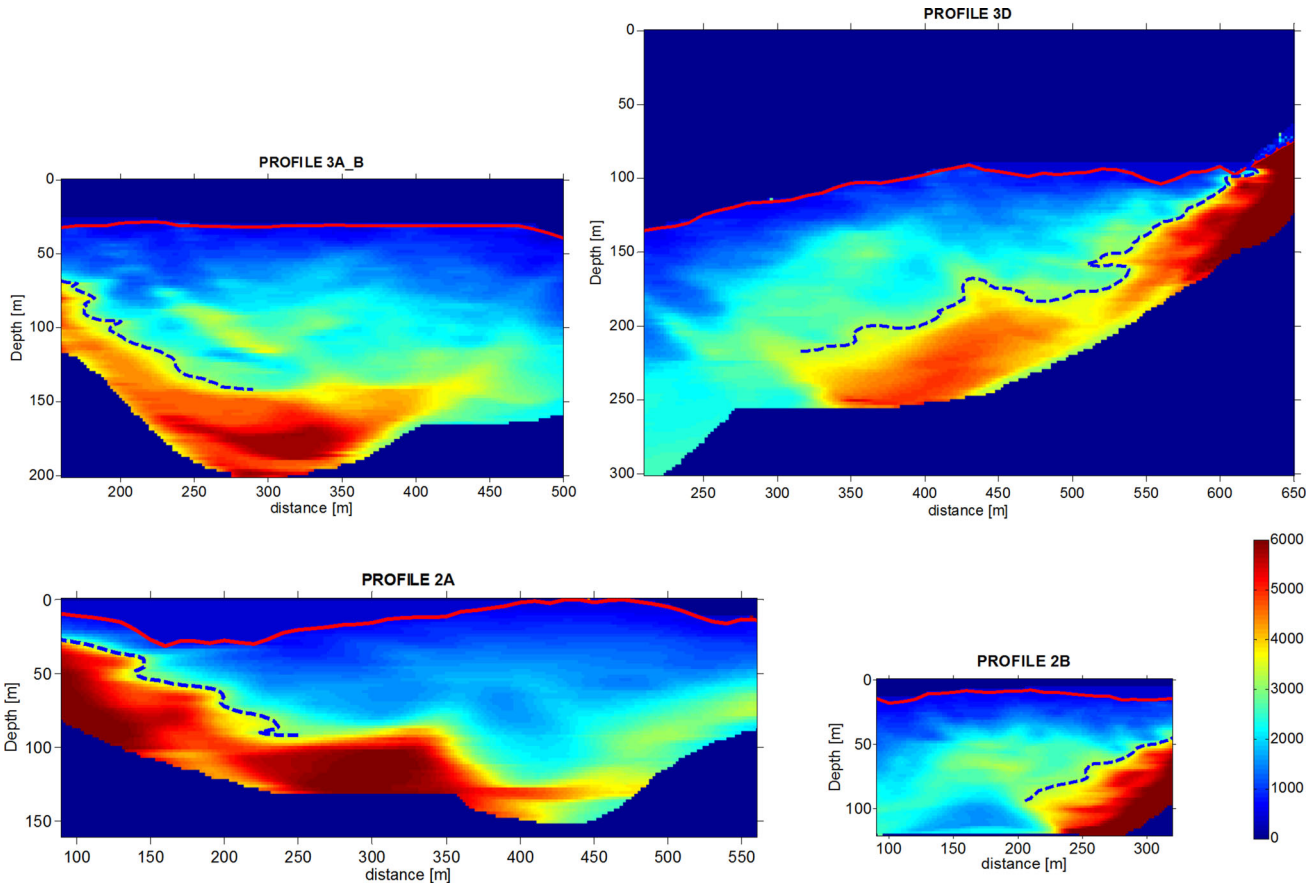

Fig. 6 Seismic refraction tomography velocity sections (velocities are in m/s and null velocity means areas not visited by source-receiver travel paths). *Solid red lines* are topography and *dashed blue lines* represent the picked interfaces

during this occurrence. The simulated outcomes were then compared to movements recorded by the geotechnical monitoring network, and an evaluation among the outputs of two models was carried out to determine the code providing the best fit.

Rock mass characterization

A rock mass geomechanical characterization was conducted in order to define the input parameters for the numerical simulations. Geomechanical parameters were determined considering the properties of both the discontinuities and the intact rock (Sitharam et al. 2001, 2007). All available information was gathered together to obtain a suitable evaluation of the mechanical properties of the rock mass. Common rock mass quality assessment methods, such as Rock Quality Designation (RQD) and Geological Strength Index (GSI), were initially performed on the brecciated and fractured area and on the intact rock (bedrock). Starting by the borehole loggings analysis, the RQD index was determined. The landslide body is composed by rocks belonging to the Gneiss formation of Monte Canale, an ortogneiss with mica schists characterize by RQD value less than 10 %. The thickness of this layer ranges from 60 to 100 m, but in some spots it is as thick as 120 m. Beyond this layer, gneiss with schists with RQD value higher than 75 % was detected (Belloni and Gandolfo 1997).

During the geological and structural surveys, several field observations on the outcrop and in the explorative tunnel were collected. A quantitative way to transfer these data into a rock mass quality is offered by the GSI (Hoek and Brown 1997; Marinos et al. 2005). Several applications of GSI to landslide stability analysis have been published in the literature, and some authors recently discussed the limitations of this method (Brown 2008; Brideau et al. 2009). A common problem of this approach regards the limited view presented by the outcrop. This is not an issue for Spriana landslide because the presence of the explorative tunnel offers the unusual possibility to explore the inner structure of the slope. GSI values of Spriana rock mass are presented in Fig. 7. As for many other complex landslides (Brideau et al. 2012), fractured and brecciated rocks in the whole landslide body were assigned a GSI of 20–30, while bedrock was assigned a range of values

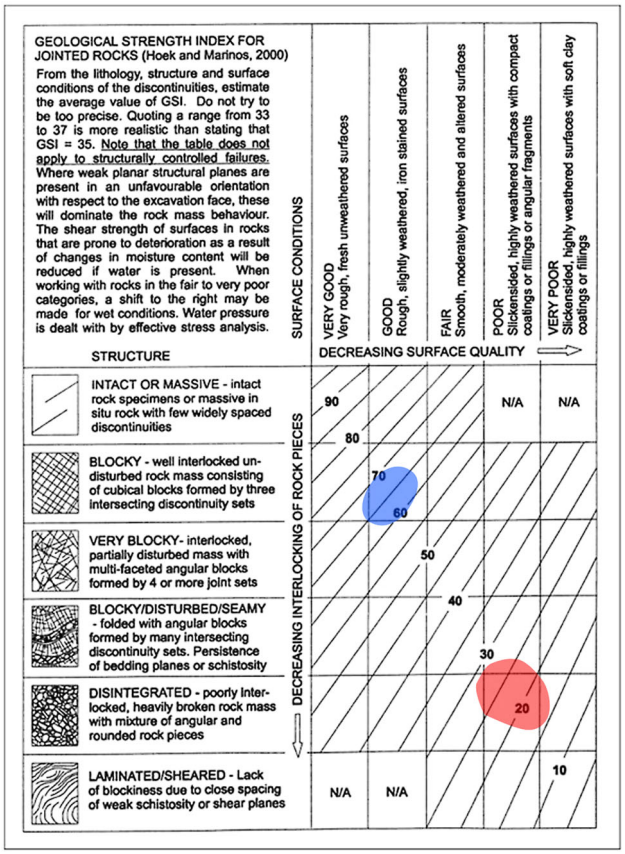

Fig. 7 Range of GSI for Spriana rock mass (modified after Marinos et al. 2005)

spanning from 65 to 75. After this analysis, laboratory tests conducted on the rock samples collected in the explorative tunnel allowed quantitative characterization of the fault zone. The results of direct shear tests are reported in Table 1. Unfortunately, the deep failure surface affecting the northern section of the slope (near Bedoglio Valley) was characterized only according to literature values because no direct samples of this weak surface were available. It is indeed true that the effectiveness of the numerical simulations presented in the following could be improved after ad hoc laboratory tests of the material of this surface. Among several case studies presented in the scientific literature, the authors deemed it reasonable to consider the Downie Slide, because it is composed by highly fractured, inter-layered schist, gneiss and quartzite (Kalenchuk et al. 2013). Table 1 lists the geomechanical parameters of the whole slope, considering the bedrock, the fractured rock (landslide body) and the failure surface (fault zone and weak layer).

Three-dimensional modelling

The three-dimensional finite difference model FLAC3D (Itasca 2005) was used to assess the role of the fractured and brecciated rocks in the landslide body. Indeed, such a discontinuous heterogeneous and anisotropic rock mass usually requires the assumption of an equivalent continuum numerical approach. Despite FLAC3D being based on a continuous approach, shear planes can also be included. Therefore, the shear surface resulting from the intersection of the two weak zones was taken into account. The three-dimensional distinct element code 3DEC (Itasca 2008) was used to assess the role of the geometry of the shear surface on the slope stability. In this case, the blocks can be modelled as rigid or deformable. While the two intersecting planes of the failure surface are well accounted for using this discontinuous approach, on the other hand it is necessary to consider deformable blocks to simulate the fractured rock mass of the landslide body. Both models, FLAC3D and 3DEC, assume that rock mass behaves as an elasto-plastic Mohr–Coulomb material.

The outcomes of the two numerical approaches are reported in Fig. 8. Both codes correctly reproduce the displacements observed in the monitoring data sets, and both simulations display greater displacements in the southern section of the slope. FLAC3D locates displacements on the shear surface at the side of the fault zone and shows comparable behaviors of the fault zone and of the landslide body (Fig. 8). A wedge-shaped movement is more evident in the

Table 1 Mechanical properties for FLAC 3D and 3DEC models

	Model	Density (kg/m^3)	K (Pa)	G (Pa)	φ (°)	Cohesion (Pa)
Rock mass						
Fractured and brecciated rock mass	Mohr–Coulomb	2,800	3.0e8	1.9e8	34	1e6
Bed Rock	Mohr–Coulomb	2,800	29e9	13.5e9	44	14.5e6

	Model	K_n (Pa/m)	K_s (Pa/m)	φ (°)	Cohesion (Pa)	Tensile strength (Pa)
Surface of failure						
Fault	Mohr–Coulomb	10e6	5e6	24	0.5e4	–
Weak plane	Mohr–Coulomb	15e6	7.5e6	26	0.5e5	50e3

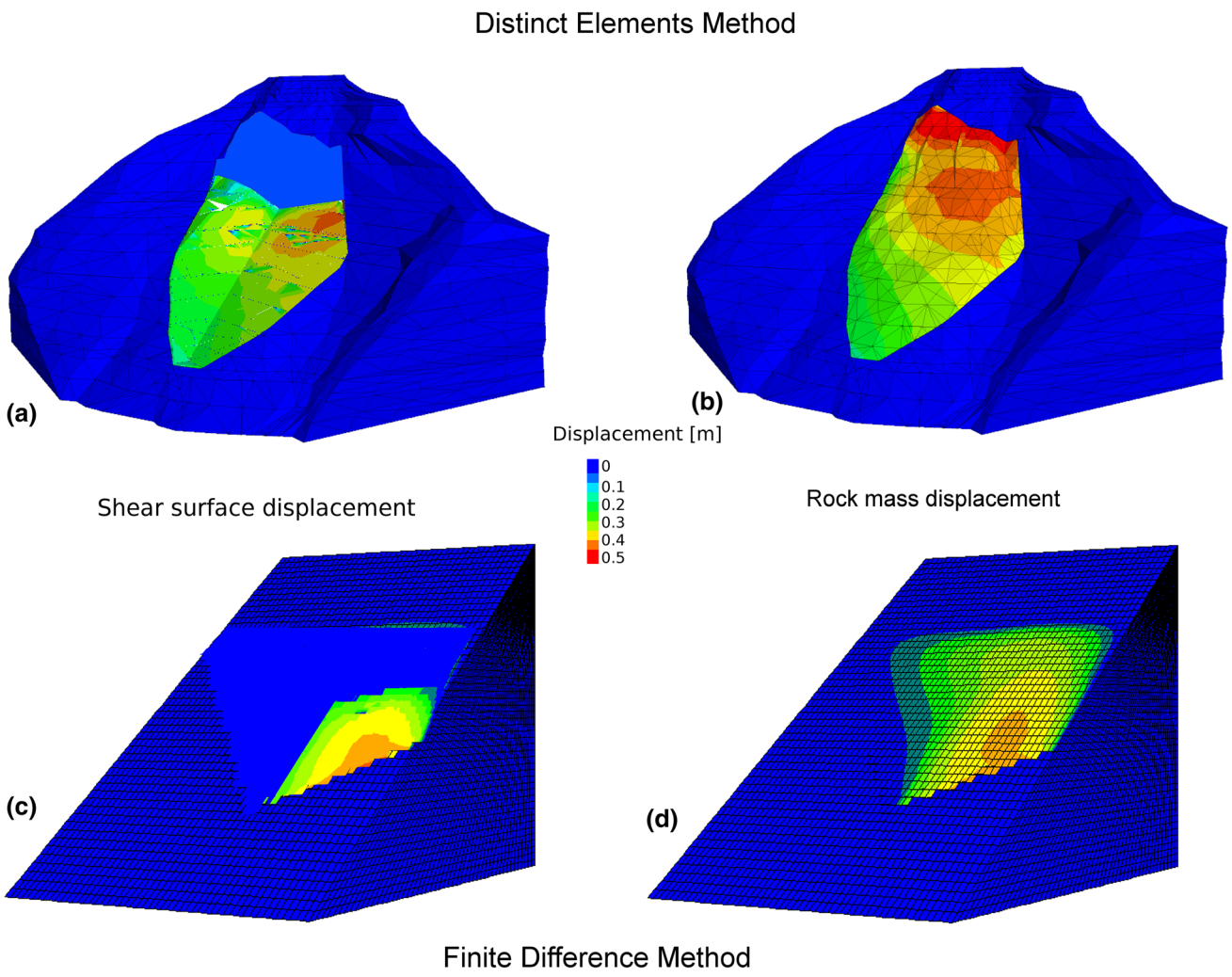

Fig. 8 Outcomes of numerical modelling

3DEC simulation, where displacements of the failure surface mainly occurring close to the fault zone cause even greater displacements along the landslide main scarp (according to extensometer E106). Moreover, in agreement with data sets recorded by inclinometers I103 and I113, greater displacements on the shear zone are recorded in the upper part. Although FLAC3D code can simulate landslide body deformation and is able to take into account the role of discontinuities, 3DEC outcomes prove that this code is able to simulate a behaviour that better fits the collected monitoring data sets. The hypothesis of the haulage of the wedge-shaped unstable body due to the fault zone movement seems to agree with the outputs of the 3DEC numerical model.

Conclusion

The primary intention of this paper was to update the geological model of a large-complex landslide in the Alpine area. Through a multidisciplinary approach, a new hypothesis on the shear surface for Spriana landslide was formulated. The geological study of the slope based on outcrop analysis, borehole loggings examination and structural survey inside the explorative tunnel suggests that the deeper sliding surface is characterized by poor mechanical properties and is located within the more fractured rock mass layer. Failure surface close to Bedoglio Valley is characterized by brecciated rock mass and has a dip direction of 180° and inclination of about 30°. Conversely, the fault zone identified near Calchera Valley is considered an important larger structural feature that controls the behaviour of the southern part of the slope. Assuming the surface of failure is composed of two different planes, the landslide body would have a wedge shape delimited on one side by a fault zone with estimated attitude 260°/25°–30°, and on the other side by the interface between fractured rock and bedrock with attitude around 180°/30°. Processing of geophysical data by means of

seismic refraction tomography supports this interpretation. According to the described geological model, the landslide volume can be estimated to be around 50 millions of cubic metres. Only the shear surface along the fault zone seems to have already undergone complete failure, as response to the triggering factors is immediate. In case of movements, the southern section probably pulls the northern section, close to Bedoglio Valley, that is most likely still bound to the slope and presents higher shear strength. The gradual failure of this section may be corroborated by the lower but more continuous displacements that occurred during heavy rainfall events. A structurally controlled, wedge-like rockslide is proposed by the authors. Moreover, besides the complex geological setting, considering the steepness of the slope, the degree of fracturation of the rock mass, the presence of a less inclined surface of failure and the foot located at higher altitude than the valley, the landslide may change into a rock-debris avalanche in the case of heavy rainfalls taking place.

The updated physical model of the slope was tested using numerical modelling to perform a back analysis of the 2001 event. Both continuous and discontinuous modelling approaches gave results in agreement with the collected monitoring data sets, but the distinct element code provided a better understanding of the wedge-shaped structure. The authors believe that further simulations should be performed to study the response of the modelled landslide body according to variations of the input parameters (e.g., groundwater table level).

Acknowledgments The authors wish to thank Ing. Antonella Caimi, Dott. Gregorio Mannucci, Dott. Leonardo La Rocca and Dott. Alessandro Ballini for their assistance in field investigations. The help of Ing. Valentina Melillo is also acknowledged. The comments and suggestions of two anonymous reviewers significantly improved the quality of this manuscript.

References

Aleotti P, Chowdury R (1999) Landslide hazard assessment: summary review and new prospective. Bull Eng Geol Environ 58(1):21–44

Ballantyne C-K (2002) Paraglacial geomorphology. Quat Sci Rev 2:1935–2017

Belloni L, Gandolfo M (1997) La frana di Spriana. Geologia tecnica ed ambientale 3:7–36 (in Italian)

Bonnard C, Dewarrat X, Noverraz F (2004) The Sedrun landslide. In: Bonnard C, Forlati F, Scavia C (eds) Identification and mitigation of large landslide risks in Europe: advances in risk assessment. IMIRILAND Project. Balkema, Leiden, pp 227–252

Brideau M-A, Yan M, Stead D (2009) The role of tectonic damage and brittle rock fracture in the development of large rock slope failures. Geomorphology 103(1):30–49

Brideau M-A, McDougall S, Stead D, Evans GS, Couture R, Turner K (2012) Three-dimensional distinct element modelling and dynamic runout analysis of a landslide in gneissic rock, British Columbia, Canada. Bull Eng Geol Environ 71(3):467–486

Brown ET (2008) Estimating the mechanical properties of rock masses. In: Potvin Y, Carter J, Dyskin A, Jeffrey R (eds) SHIRMS 2008. Australian Centre for Geomechanics, Perth, pp 3–22

Brugner W (1961) Sul movimento franoso nel territorio di Spriana. Servizio Geologico d'Italia (in Italian)

Brugner W (1963) Ulteriori osservazioni sulla frana di Spriana. Servizio Geologico d'Italia (in Italian)

Brugner W (1964) Primo esame di cunicoli in corso d'opera nella frana di Spriana. Servizio Geologico d'Italia (in Italian)

Calvetti F, Crosta GB, Tatarella M (2000) Numerical simulation of dry granular flows: from the reproduction of small-scale experiments to the prediction of rock avalanches. Rivista Italiana di Geotecnica 2:21–38

Campbell CS, Cleary PW, Hopkins M (1995) Large-scale landslides simulations: global deformation, velocities and basal friction. J Geophys Res 100(B5):8267–8283

Cancelli A (1986) Problemi geologico-tecnici della frana di Spriana. Atti del Convegno Valmalenco. Natura 1, 27–29 sett. 1986:158–176 (in Italian)

Cancelli A, Coffano F, Villa F (1979) Relazioni sulle indagini eseguite e eseguende con riferimento alla frana di Spriana. Commissione tecnica Regionale per la frana di Spriana (in Italian)

Catane SG, Cabria HB, Zarco MAH, Saturay RM Jr, Mirasol-Robert AA (2008) The 17 February 2006 Guinsaugon rock slide-debris avalanche, Southern Leyte, Philippines: deposit characteristics and failure mechanism. Bull Eng Geol Environ 67(3):305–320

Crosta GB, Calvetti F, Imposimato S, Roddeman D, Frattini P, Agliardi F (2001) Granular flows and numerical modelling of landslides. Report of DAMOCLES project August 2001, CNR

Crosta GB, Imposimato S, Roddeman DG (2003) Numerical modeling of large landslides stability and runout. Nat Hazards Earth Syst Sci 3:523–538

Cruden DM, Varnes DJ (1996) Landslide investigation and mitigation. Special report 247, vol 3. Transportation Research Board US National Research Board, US National Research Council, Washington DC, pp 36–75

Cundall PA (1971) A computer model for simulating progressive, large-scale movements in blocky rock systems. In: Proceedings of the international symposium on rock fracture, Nancy, II-8

Dai FC, Lee CF, Ngai YY (2002) Landslide risk assessment and management: an overview. Eng Geol 64(1):65–87

Discenza ME, Esposito C, Martino S, Petitta M, Prestininzi A, Scarascia Mugnozza G (2011) The gravitational slope deformation of Mt. Rocchetta ridge (central Apennines, Italy): geological-evolutionary model and numerical analysis. Bull Eng Geol Environ 70:559–575

Eberhardt E, Stead D, Coggan JS (2004) Numerical analysis of initiation and progressive failure in natural rock slopes—the 1991 Randa Rockslide. Int J Rock Mech Min Sci 41(1):69–87

Einstein HH (1988) Special lecture: landslide risk assessment procedure. In Bonnard C (ed) Proceedings of the 5th international symposium on landslides, Lausanne (CH) 10–15 July 2, pp 1075–1090

Fukawa T, Ohnishi Y, Nishiyama S, Uehara S, Miki S (2005) Three dimensional discontinuous deformation analysis for rockfall simulation. In: Barla G, Barla M (eds) 11th IACMAG conference, pp 513–520

Futalan KM, Biscaro JRD, Saruray RM, Catane SG, Amora MS, Villaflor EL (2010) Assessment of potential slope failure sites at Mt. Can-abag, Guinsaugon, Philippines, based on stratigraphy and rock strength. Bull Eng Geol Environ 69:517–521

Gattinoni P, Scesi L, Arieni L, Canavesi M (2012) The February 2010 large landslide at Maierato, Vibo Valentia, Southern Italy. Landslides 9:255–261

Gonzales E, Herreros MI, Pastor M, Quecedo M, Fernandez Merodo JA (2003) Discrete and continuum approaches for fast landslide modelling. In: Konietzky H (ed) 1st International symposium on numerical modeling in micromechanics via particle methods, Swets and Zeitlinger, Lisse, pp 307–313

Hoek E, Brown ET (1997) Practical estimates of rock mass strength. Int J Rock Mech Min Sci 34(8):1165–1186

Howard KA (1973) Avalanche mode of motion: implications from lunar examples. Science 180:1052–1055

Hsu K (1975) Catastrophic debris streams (sturzstroms) generated by rockfalls. Geol Soc Am Bull 86:129–140

Hungr O, Corominas J, Eberhardt E (2005) Estimating landslide motion mechanism, travel distance and velocity. In: Hungr O, Fell R, Couture R, Eberhardt E (eds) Landslide risk management. Taylor & Francis Group, Vancouver, pp 99–128

International Society of Rock Mechanics ISRM (1978) Suggested methods for the quantitative description of discontinuities in rock masses. Int J Rock Mech Min Sci Geomech Abstr 15:319–368

Istituto Sperimentale Modelli e Strutture ISMES - Cogefar- Cariboni (1990a) Frana di Spriana: Indagini ed ulteriori studi nel versante in frana. Cunicolo Esplorativo (in Italian)

Istituto Sperimentale Modelli e Strutture ISMES - Cogefar- Cariboni (1990b) Frana Spriana: Rapporti Complementari. Aree di invasione della frana. Rapporto finale (in Italian)

Itasca (2005) Flac 3D user's manual. Itasca Consulting Group Inc., Minnesota

Itasca (2008) 3DEC user's guide. Itasca Consulting Group Inc., Minnesota

Jing L, Hudson JA (2002) Numerical methods in rock mechanics. Int J Rock Mech Min Sci 39:409–427

Kalenchuk KS, Hutchinson DJ, Diederichs MS (2013) Downie Slide: numerical simulation of groundwater fluctuations influencing the behavior of a massive landslide. Bull Eng Geol Environ 72:397–412

Koo CY, Chern JC (1998) Modification of the DDA method for rigid block problems. Int J Rock Mech Min Sci 35(6):683–693

Geoprospecting s.r.l (1990) Indagine geofisica mediante sismica a rifrazione eseguita in località Case Cucchi nel Comune di Spriana (SO) (in Italian)

Longoni L, Papini M, Brambilla D, Arosio D, Zanzi L (2013) The role of shear surface geometry in the definition of deep seated gravitational slope deformation thresholds. In: Kwasniewski M, Łydzba D (eds) Rock mechanics for resources, energy and environment. Taylor & Francis Group, London, pp 654–658

Marcato G, Silvano S, Zabuski L (2005) Modellazione di ammassi rocciosi instabili con il metodo degli elementi distinti. Giornale di Geologia Applicata 2:87–92 (in Italian)

Marinos V, Marinos P, Hoek E (2005) The geological strength index: applications and limitations. Bull Eng Geol Environ 64(1):55–65

Palmer D (1981) An introduction to the generalized reciprocal method of seismic refraction interpretation. Geophysics 46:1508–1518

Papini M, Mannucci G, Longoni L, Caimi A (2005) Il ruolo delle rocce deboli nella definizione del modello fisico della frana di Spriana. Quaderni di Geologia Applicata 12(2):57–70 (in Italian)

Phillips WS, Fehler MC (1991) Travel time tomography: a comparison of popular methods. Geophysics 56:1639–1649

Pirulli M (2009) The Thurwieser rock avalanche (Italian Alps): description and dynamic analysis. Eng Geol 109:80–92

Revellino P, Hungr O, Guadagno FM, Evans SG (2004) Velocity and runout simulation of destructive debris flow and debris avalanches in pyroclastic deposits, Campania region, Italy. Environ Geol 45:295–311

Savage SB, Hutter K (1989) The motion of a finite mass of granular material down a rough incline. J Fluid Mech 199:177–215

Scavia C, Barla G, Bernaudo V (1990) Probabilistic stability analysis of block toppling failure in rock slopes. Int J Mech Min Sci Geomech Abstr 27(6):465–478

Scheiddeger A (1973) On the prediction of the reach and velocity of catastrophic landslides. Rock Mech 5:231–236

Shi GH (1988) Discontinuous deformation analysis—a new numerical model for the static and dynamics of block systems. Phd Dissertation; Depth Civil Engineering. University of California Berkeley

Sitharam TG, Sridevi J, Shimizu N (2001) Practical equivalent continuum characterization of jointed rock masses. Int J Rock Mech Min Sci 38:437–448

Sitharam TG, Maji VB, Verma AK (2007) Practical equivalent continuum model for simulation of jointed rock mass using FLAC 3D. Int J Geomech 7:389–395

Stead D, Eberhardt E, Coggan JS (2006) Developments in the characterization of complex rock slope deformation and failure using numerical modeling techniques. Eng Geol 83:217–235

Telford WM, Geldart LP, Sheriff RE (1990) Applied geophysics, 2nd edn. Cambridge University Press, Cambridge

Tian Chi L (1983) A mathematical model for predicting the extent of a major rockfall. Zeitschrift fuer Geomorphologie 4:473–482

Tommasi P, Consorti C, Campedel P, Ribacchi R (2003) Analysis of rock avalanches generated by planar rock slides on high mountain slopes. In: Picarelli L, Cascini L (eds) International conference on fast slope movements Naples, pp 503–510

Tommasi P, Campedel P, Consorti C, Ribacchi R (2008) A discontinuous approach to the numerical modelling of rock avalanche. Rock Mech Rock Eng 41:37–58

Welkner D, Eberhardt E, Hermanns RL (2010) Hazard investigation of the Portillo Rock Avalanche site, Central Andes, Chile, using an integrated field mapping and numerical modelling approach. Eng Geol 114:278–297